Int. J. Electrochem. Sci., 7 **(2012)** 4871 - 4888

International Journal of
ELECTROCHEMICAL
SCIENCE
www.electrochemsci.org

Synthesis and Catalytic Activity of TiO_2 Nanoparticles for Photochemical Oxidation of Concentrated Chlorophenols under Direct Solar Radiation

Muneer M. Ba-Abbad[1,*], *Abdul Amir H. Kadhum*[1], *Abu Bakar Mohamad*[1], *Mohd S. Takriff*[1], *Kamaruzzaman Sopian*[2]

[1] Department of chemical and process Engineering, Faculty of Engineering and Built Environment, Universiti Kebangsaan Malaysia, 43600, Bangi, Selangor Darul Ehsan, Malaysia
[2] Solar Energy Research Institute (SERI), Universiti Kebangsaan Malaysia, 43600, Bangi, Selangor Darul Ehsan, Malaysia
[*]E-mail: muneer711@gmail.com

Received: 28 February 2012 / *Accepted:* 14 May 2012 / *Published:* 1 June 2012

The titanium dioxide (TiO_2) nanoparticles catalyst was synthesized via sol-gel method using the titanium tetra-isopropoxide as starting material. The effects of calcination temperatures on the crystalline structure, surface area and photocatalytic activity of TiO_2 nanoparticles were investigated. The anatase to rutile percentage decreases when temperatures greater than 500^{o}C and evaluated from XRD intensity of (101) and (110) peak, respectively. Photocatalytic activity of TiO_2 nanoparticles was tested by the degradation of chlorophenols namely, 2-chlorophenol (2-CP), 2, 4-dichlorophenol (2,4-DCP) and 2, 4,6-trichlorophenol (2,4,6T-CP) within range from 50 to 150 mgl^{-1} initial concentrations under direct solar radiation. The results of photodegradation, 99, 98 and 92 % was obtained for 50 mgl^{-1} of 2-CP, 2,4-DCP and 2,4,6-TCP receptively after 90 min irradiation time at pH of 6. At the same time, the efficiency value was decreased with initial concentration more than 50 mgl^{-1}. The chemical oxygen demand (COD) removal follows the photodegradation in behavior was observed. The kinetic studies indicate that the reaction was following to first order and decrease of rate constant (K_{app}) with initial concentration more than 50 mgl^{-1}.

Keywords: Solar Photocatalytic, Chlorophenols, TiO_2 nanoparticles, Sol-gel.

1. INTRODUCTION

The oxide nanoparticles synthesized by several methods appears more and more useful because these nanoparticles have good electrical, optical and magnetic properties that are different from their bulk counterparts [1]. Titania nanoparticles have received much interest for applications such as

optical devices, sensors, and photocatalysis [2, 3]. There are several factors in determining important properties in the performance of TiO_2 for applications such as particle size, crystallinity and the morphology [4-6]. The presence of chlorinated compounds in aquatic environments has caused severe environmental pollution problems. 2-chlorophenol and 2, 4-dichlorophenol are typical phenolic substances has been used as an intermediate in making insecticides, herbicides, preservatives, antiseptics, disinfectants and other organic compounds [7]. 2,4,6-trichlorophenol is particularly of environmental interest owing to its mutagenicity and carcinogenicity [8]. Traditional wastewater treatment techniques consist of activated carbon adsorption and biological digestion. Each of these techniques has limitations and disadvantages. For activated carbon adsorption only involves the phase transfer of pollutants without decomposition thus introduces another pollution problem [9]. On the other hand, in biological treatment, the decomposition of many chlorinated phenols have proven inefficient since chlorinated phenols are resistant to biodegradation within an acceptable time period and tend to accumulate in sediments [10,11]. Chlorophenols do not undergo direct sunlight photolysis in the natural environment since they only absorb light below 290 nm [12]. Therefore, the advanced oxidation processes (AOP) appears to be a good method for destruction the toxic pollutants into nontoxic substances [13]. Photocatalytic oxidation reactions are initiated when a photon of higher energy level or equal to the band gap energy is absorbed by a TiO_2 catalyst promoting an electron (e^-) from the valence band to the conduction band with simultaneous generation of a positive hole (h^+) in the valence band [14]. The mechanism of radical's generation ($^{\bullet}OH$ and $^{\bullet}O_2^-$) is presented as follows [15]:

$$TiO_2 + h\nu \rightarrow TiO_2(e^- + h^+) \quad (1)$$

$$H_2O + TiO_2(h^+) \rightarrow TiO_2 + {}^{\bullet}OH + H^+ \quad (2)$$

$$O_2 + TiO_2(e^-) \rightarrow TiO_2 + {}^{\bullet}O_2^- \quad (3)$$

TiO_2 nanocatalyst was synthesized by a simple sol gel method. The structure and morphology of the synthesized nanocrystalline TiO_2 were characterized by XRD, FESEM,TEM, and BET. The effect of some parameters such as annealing temperature, catalyst loading, and initial concentration of chlorophenols were investigated.

2. EXPERIMENTAL AND METHODS

2.1. Materials

Tetraisopropoxide (purity, 97%), Ti $[OC_3H_7]_4$ was used as a starting material and supplied by sigma-Aldrich company. Ethanol $[C_2H_6O]$ was obtained from BDH Prolabo chemicals and nitric acid $[HNO_3]$ from Merck. De-ionized water was used for preparing all standard solutions. 2-chlorophenol and 2,4,6-trichlorophenol were obtained from Merck, and 2,4-dichlorophenol from Sigma-Aldrich.

2.2. Preparation of TiO_2 nanoparticles

TiO_2 nanoparticles were synthesized by hydrolyzing titanium tetra isopropoxide (TTIP) in a mixture of ethanol and water. All procedures of synthesis of TiO_2 nanoparticles were reported in our previous study [16]. The final gel was dried at 80^{o}C for 4 hr. Finally, the white powder was calcined at different temperatures 400, 500, 600, 700^{o}C and the activities of TiO_2 samples on degradation of chlorophenols under direct solar radiation were evaluated.

2.3. Characterization of TiO_2 nanoparticles

The thermal-decomposition behavior of the dry gel was monitored using a TGA, (model STA 449F3, Jupiter, Netzsch, Germany). The crystal phase composition and the crystallite size of the TiO_2 nanoparticles, was recorded using X-ray diffraction (XRD) (Brukur D8 Advance AXS) with CuKα radiation (1.5406 Å) in the 2θ scan range of 20-80°. The morphology and structure of the particles were investigated using field emission scanning electron microscopy (SUPRA 55VP) and transmission electron microscope (JEOLJEM 2100) with an acceleration voltage of 200kV. The specific surface area (BET) was determined using Micromeritics ASAP 2020 Accelerated Surface Area & Porosimetry System. The absorption spectra of the TiO_2 samples were measured by UV/Vis spectrophotometer equipped (Perkin Elmer (lambda 35) with an integrating sphere. The baseline correction was performed using a calibrated sample of barium sulfate, and the spectra were recorded at room temperature in air in the range of 200–600 nm.

2.4. Photocatalytic degradation procedures

Photodegradation experiments of chlorophenols were conducted in a slurry batch reactor. All of the experiments were carried out under similar conditions on sunny days at times between 11.00 a.m. and 2.30 p.m. All photocatalytic experiments were applied at ambient temperature (28-38°C). A 100 ml of 50 mgl^{-1} chlorophenols with 100-300 mgl^{-1} of TiO_2 nanoparticle were used to determine the optimum loading. It was placed in the dark condition for 60 min with continuous stirring for adsorption–desorption equilibrium and then exposed to sunlight. Every 15 min as interval time a sample was withdrawn, centrifuged and filtered. The filtered samples was analyzed using an Agilent (1200 HPLC) in which a Jones LC-18 column (250mm x 4.6mm x 4µm), with a variable wavelength UV detector. An acetonitrile: water (20:80 v/v) with 0.01M phosphoric acid (H_3PO_4) as a mobile phase and flow rate of 1.0 ml min^{-1} was used. Sample with a volume of 20 µL was used as injection volume and concentration of 2-chlorophenol, 2,4-dichlorophenol and 2,4,6-trichlorophenol were evaluated by UV detector at wavelength 254, 284 and 293 nm, respectively. The Photocatalytic degradation was calculated as follows:

$$\text{Photocatalytic degradation \%} = \left(\frac{Co - C}{Co}\right) \times 100 \quad (4)$$

where C_o is the initial concentration and C, is the concentration of 2-chlorophenol at intervals of the irradiation time. The COD tests were carried out according to close reflux, colorimetric method [17] using Hach DR/2010 Spectrophotometer and Hach COD reactor.

2.5. Intensity of solar light

The UV intensity of solar light was recorded for all experiments under similar conditions on sunny days. The intensity was measured for every 5 min and average over the period of experiments was 23 Wm^{-2} and almost constant. The UV intensity was measured by a Skyelynx type SDL 5100.

3. RESULTS AND DISCUSSION

3.1. Characterization of the TiO_2 nanoparticles

3.1.1. Thermal Analysis

Fig. 1 shows TGA curve of TiO_2 precursor after drying at 80°C for 4 hr. Three main stages of TGA curve of TiO_2 sample according to the heat profile were observed. The temperature increases from 25 to 180 °C as first stage, which is assigned to remove the remaining ethanol, water and about 14 % weight loss was occurred. In the range of temperature of 180 to 380 °C, is attributed to decomposition of the organic compounds completely with about 9.0 % weight was lost [18]. The amorphous precursor was converted to anatase phase as the temperature increases from 425 to 500°C. The TiO_2 anatase was transferred to rutile phase between 550 to 600°C [19]. These observations were confirmed by XRD results as shown in Fig.2.

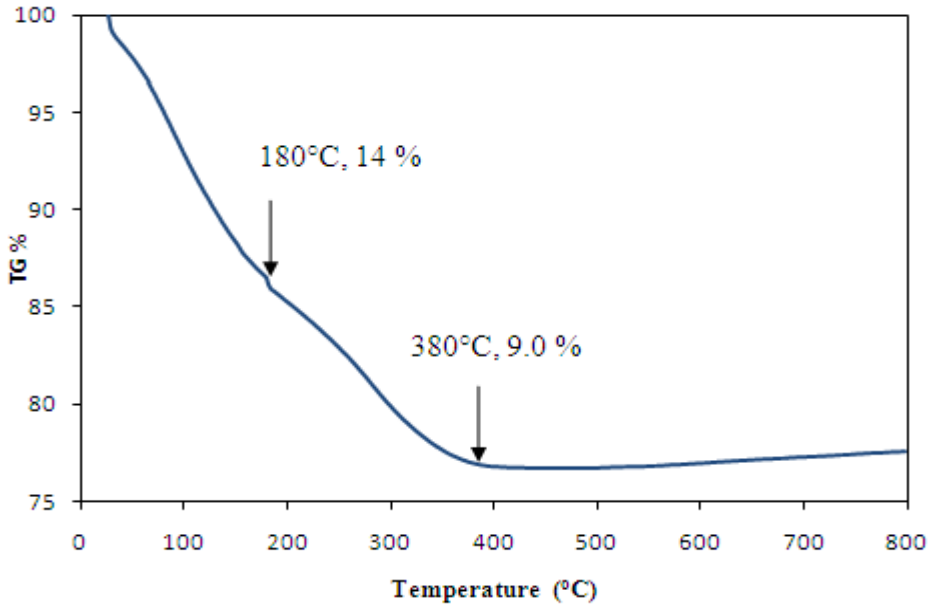

Figure 1. TGA curve of TiO_2 precursor

There is no weight loss on TGA curve after 400 °C indicating that decomposition of TiO_2 precursor has completed and can start as a first calcination temperature. Also, the results are in good agreement with the FT-IR analysis that discussed in 3.2.4 section.

3.1.2. X-ray diffraction (XRD)

The phase composition and the crystallite size of the prepared TiO_2 samples were evaluated by X-ray diffraction analysis. Fig. 2 presents the XRD patterns of calcined TiO_2 powder at different temperatures 400, 500,600 and 700^oC respectively. The peaks of samples at 400 and 500^oC were identified by comparison with JCPDS-84-1286 according 2θ which confirmed that an anatase structure at 2θ=25.4^o. It is noteworthy that the diffractograms of the samples do not present any peak assigned to rutile phase (2θ=27.36 ^{o}).

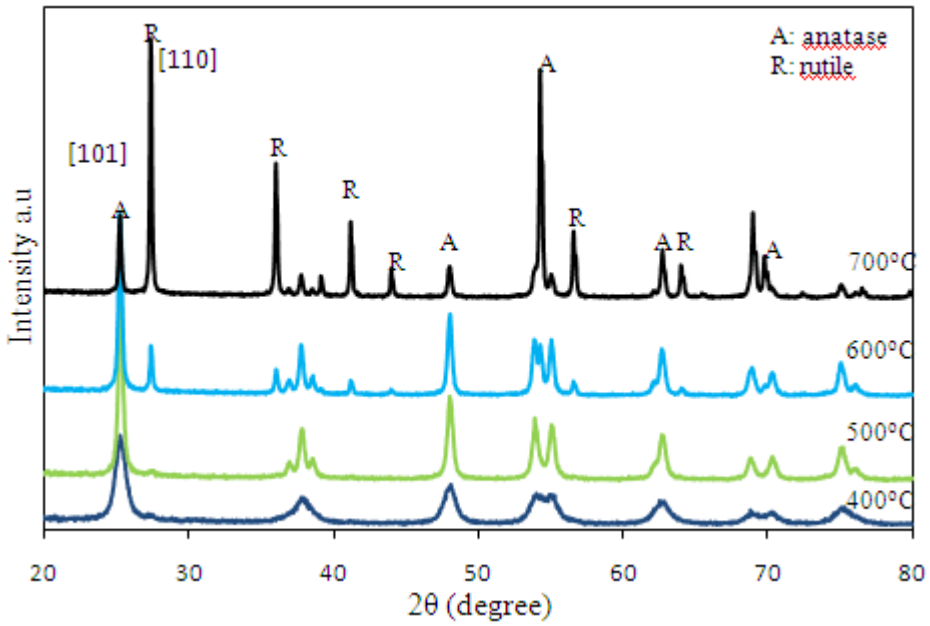

Figure 2. XRD pattern of the TiO_2 powder at various calcining temperatures.

Average crystallite size of TiO_2 was estimated according to the Scherrer's equation [20] as follows the Eq. (5):

$$D = K\lambda/\beta\cos\theta \quad (5)$$

K is the Scherer constant, λ the X-ray wavelength, β, the peak width of half maximum, and θ is the Bragg diffraction angle. The content of anatase and rutile of all TiO_2 samples was calculated as following Eq. (6):

$$X_A = 100/(1+1.265I_R/I_A) \quad (6)$$

Where X_A is the weight fraction of anatase in the mixture, I_A and I_R is intensity of anatase (101) and rutile (110) diffraction, respectively [21].

From XRD spectrum of TiO_2 sample calcined at 400^{o}C, the anatase phase only was observed and that peaks are quite wide, which indicates incomplete crystallization because it has amorphous component. This result of TiO_2 sample is a universal feature of nanoparticles [22, 23]. When the calcined temperature increased to 500^{o}C, the crystallinity of TiO_2 was improved without any change in the anatase phase. However, the rutile peaks becomes significant when temperature increased to 600^{o}C and amount of rutile was calculated about 25.49 %. The effect of calcination temperature on the changes of anatase phase to rutile is in good agreement with the results was recorded from the thermal analysis (TGA). The amount of rutile phase was increased up to 78.68% and the peaks of rutile become sharper than anatase. The particle size increases dramatically when the phase transformation from anatase to rutile was occurred [24] as given in Table 1.

Table 1. Summary of the properties of TiO_2 nanoparticles

Calcinations Temp.	Crystalline size (nm)	Surface area(m^2/g)	Lattice parameter	Anatase (%)	Rutile (%)	Band gap
400^{o}C	10±2	56.53	a=b= 3.78520 c=9.51390	100	-	3.13
500^{o}C	19±2	34.47	a=b= 3.78520 c=9.51390	100	-	3.11
600^{o}C	25±2	26.82	a=b= 3.78520 c=9.51390	74.51	25.49	3.06
700^{o}C	50±2	16.79	a=b= 4.59330 c=2.95920	21.32	78.68	3.00

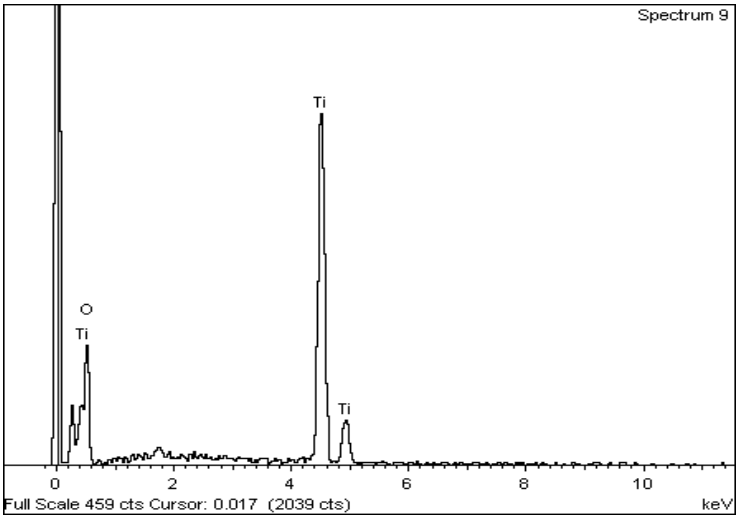

Figure 3. Energy dispersive X-ray spectrometry (EDX) of TiO_2 nanoparticle.

Energy dispersive X-ray spectrometry (EDX) analysis of TiO_2 nanoparticle at 500^oC shows peaks for Ti element and oxygen. There is no trace of any other impurities could be seen within the detection limit of the EDX as presented in Fig. 3.

3.1.3. Morphology of TiO_2 nanoparticles

Fig. 4 shows surface morphology of the TiO_2 nanoparticles at different calcination temperatures. Fig.4 (a) presents the images of TiO_2 nanoparticles calcined at 400^oC, which illustrate the small size of the particle. This result confirmed that width of the anatase peak diffraction from XRD indicating the smaller crystalline size at 400^oC. An increase the temperature up to 500^oC, the size becomes bigger than 400^oC and the agglomeration become significant. The particle size grow bigger as the calcined temperature was increased to 600^oC, which explained the effects of heat treatment on particle size of TiO_2 nanoparticles as shown in Fig.4 (b, c).

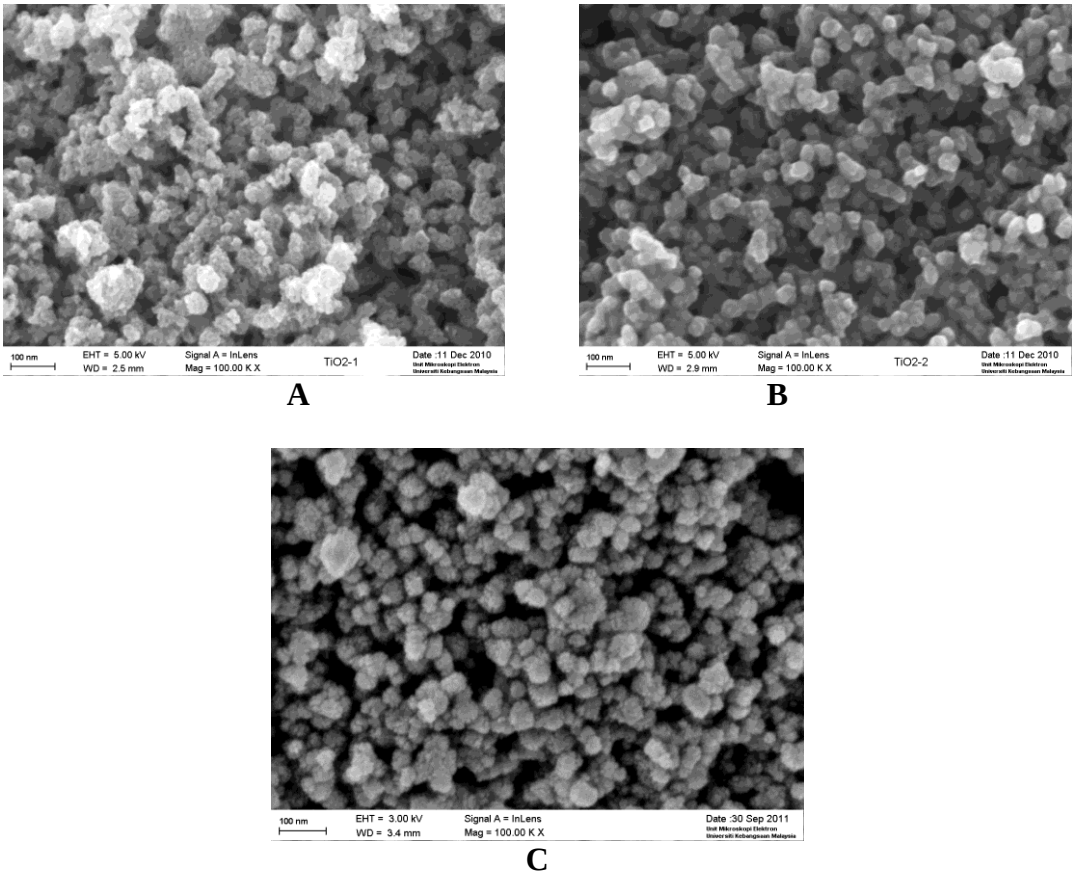

Figure 4. FESEM images of TiO_2 nanoparticles calcined at (a) 400^oC (b) 500^oC (c) 600^oC.

The particle size and shape of TiO_2 nanoparticles, which calcined at different temperature were investigated by TEM and shown in Fig.5. The TEM images illustrate that almost of the particle in spherical shape and effect of heat treatment on particle size was considerable. An increase of particle

size with calcination temperature was increased from 400 to 600^{o}C, attributed to the crystal growth. The TEM results were in good agreement with XRD data measured using Scherrer's equation and surface area data from BET as presented in Table 1.

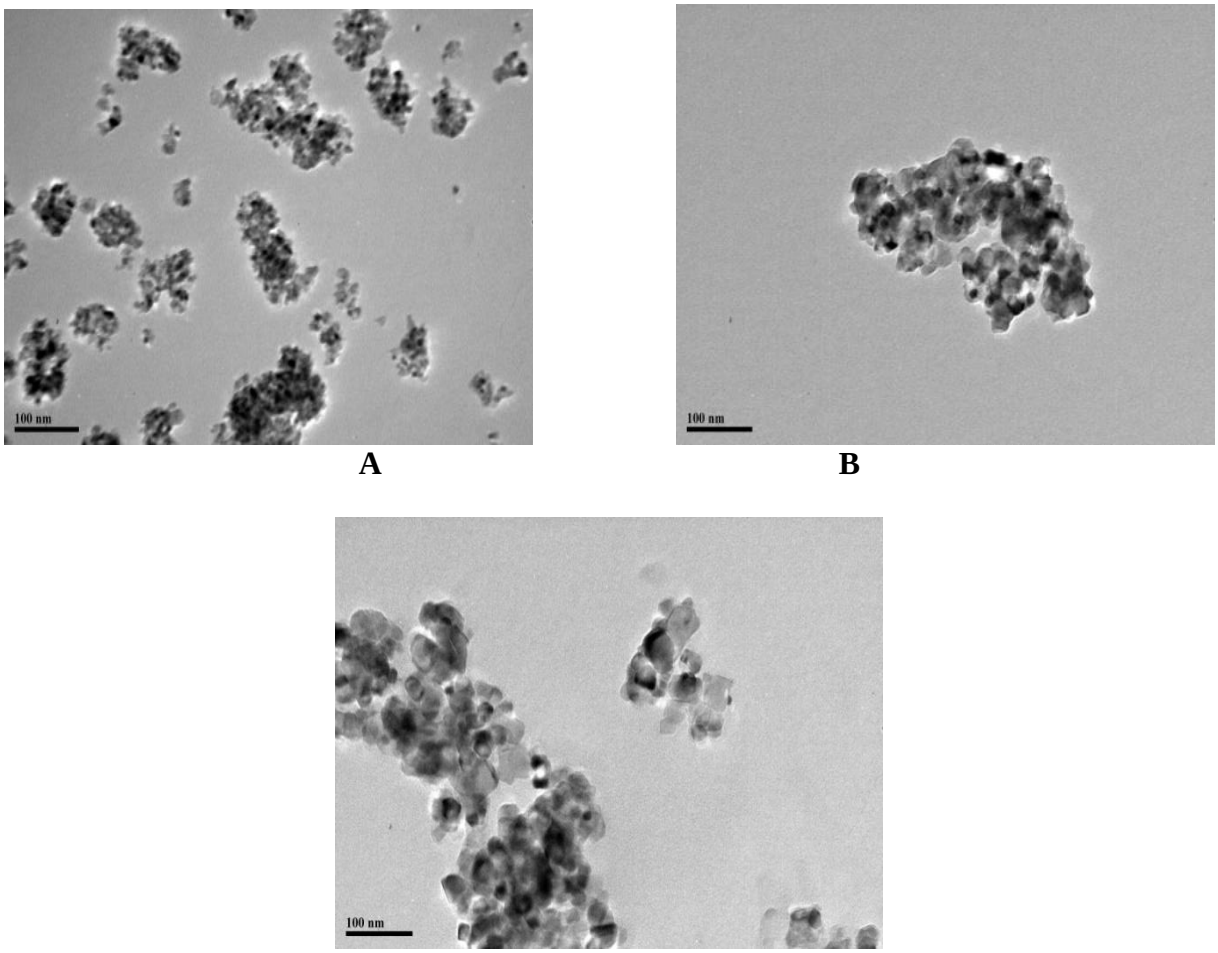

Figure 5. TEM images of TiO_2 sample calcinated at (a) 400^{o}C (b) 500^{o}C (c) 600^{o}C.

3.1.4. FT-IR of TiO_2 nanoparticles

The FT-IR spectra of TiO_2 nanoparticles as prepared and at different calcination temperatures were analyzed and given in Fig. 6. Many absorption bands belong to the organic groups such as OH and alkane were appeared. In TiO_2 as prepared sample, between 3800 to 3000 cm^{-1} a broad band was observed which related to stretching hydroxyl (O-H), representing the water as moisture. The other peaks at 1635 cm^{-1} were indicated to stretching of titanium carboxilate, which formed from TTIP and ethanol as precursors [25]. The peak between 800 and 450 cm^{-1} was assigned to the Ti-O stretching bands. After calcination of TiO_2 sample at different temperature as comparison, almost peaks of hydroxyl and carboxilate disappearance. Only the strong absorption between 800 and 450 cm^{-1} was remained, which attributed to formed of TiO_2 nanoparticles.

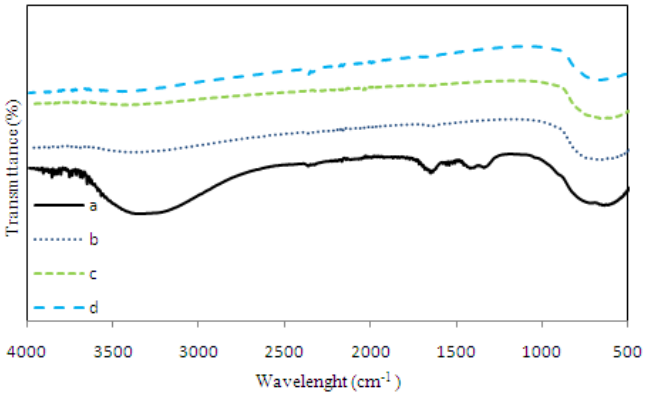

Figure 6. FT-IR spectra of (a) TiO_2 as prepared (b) 400°C (c) 500°C (d) 600°C.

3.1.5. UV-Vis analysis of TiO_2 nanoparticles

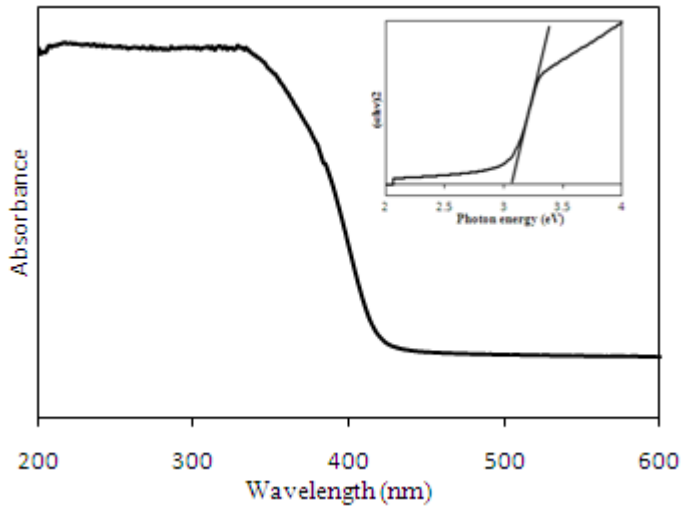

A

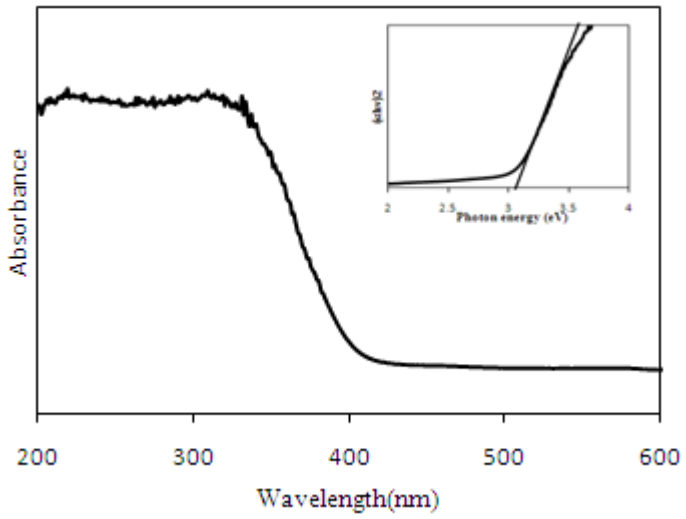

B

Figure 7. UV-Vis absorbance spectra and band gap of TiO_2 samples calcined (a) at 400°C; (b) at 500°C.

Room-temperature optical absorbance spectra of TiO_2 nanoparticles sample thermally decomposed at 400, 500 and 600^oC for 2hr are shown in Fig. 7. The absorption spectra of all TiO_2 samples exhibit strong absorption below 400 nm.

The direct band gap (E_g) of the samples is determined by fitting the absorption data to the direct transition Eq. (7):

$$\alpha h\nu = E_d(h\nu - E_g)^{1/2} \quad (7)$$

where α is the optical absorption coefficient, $h\nu$ is the photon energy, E_g is the direct band gap, and E_d is a constant[26]. The band gab of TiO_2 sample was measured by plotting $(\alpha h\nu)^2$ as a function of photon energy, and extrapolation the linear portion of the curve to absorption equal to zero as given in Fig.7. The spectrum of TiO_2 sample at 400 and 500^oC indicates the absorption onset at around 393 nm which is in excellent agreement with band gab of anatase phase [27]. When the calcination temperature increases, the band gap gradually decreased from 3.13 to 3.0 eV as reported in Table 1. At high calcined temperature of 600^oC, the band gap was at the lowest value (3.0eV) because the rutile phase and size of particle becomes bigger.

3.2 Solar photocatalytic activity of TiO_2 nanoparticles

3.2.1. Effect of radiation and dark condition on TiO_2 nanoparticles activity

The activity of TiO_2 nanoparticles on the degradation of chlorophenols was evaluated under direct sunlight.

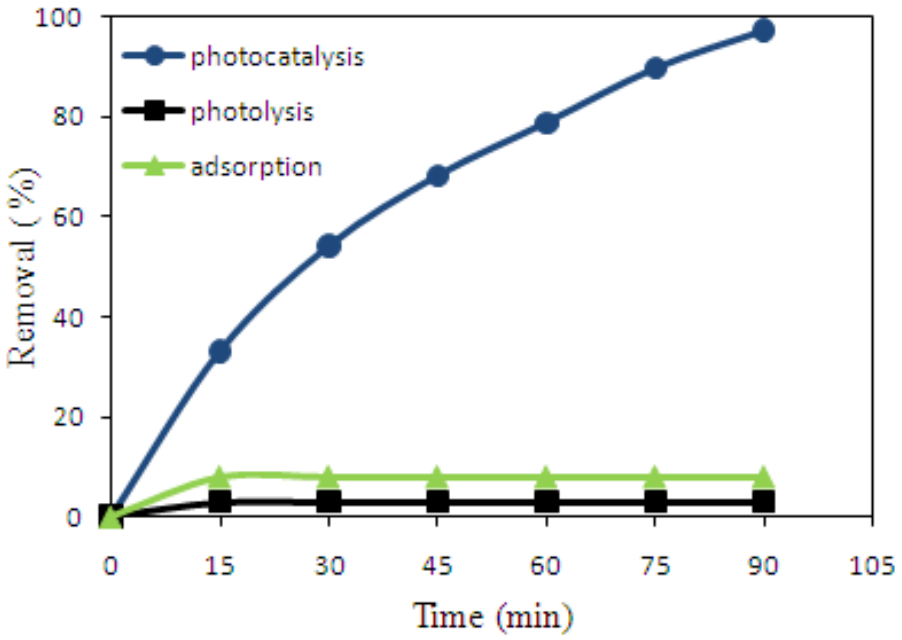

Figure 8. Comparison of photolysis, adsorption and solar photocatalysis on the removal of 2-CP (50 mg/l, Time: 90 min).

The effects of radiation and dark condition with the absence and presence of TiO_2 nanoparticles on chlorophenols removal was also studied. 2-Chlorophenol solution of 50mgl^{-1} as initial concentration was selected as the example of chlorophenol to study the effects of other parameters such as the calcintion temperatures and catalyst loading. A limited amount of 2-chlorophenol was removed under direct photolysis and in the absence of the TiO_2 nanoparticles. Further adsorption of 2-chlorophenol onto the surface of the TiO_2 under dark condition was observed after 90 min of stirring as shown in Fig. 8. A substantial amount (98.8%) of 2-chlorophenol degraded in the presence of TiO_2 nanoparticles under solar radiation.

3.2.2. Effect of calcination temperature on TiO_2 nanoparticles activity

The calcination temperature of TiO_2 samples was assigned as an important parameter effect on the performance of TiO_2 for chlorophenols degradation as shown in Fig.9. The photocatalytic activity of TiO_2 depends on main properties such as crystalline nature, phase composition and surface area as well [28]. The anatase phase of TiO_2 is considered the best active phase for degradation of organic materials than rutile [29]. The TiO_2 sample calcined at 500^{o}C indicates highest activity for 2-chlorophenol degradation which compared with 400^{o}C. The amorphous phase in nature of TiO_2 sample at 400^{o}C as shown in XRD patterns was found and may be attributed it has many imperfections and defects acts as recombination centers for the photo-formed electrons and holes [30]. At the same time, TiO_2 calcined at 500 °C, obtained well crystalline with anatase phase which resulted to higher stability and activity for 2-chlorophenol degradation. At calcination temperature of 600^{o}C, rutile phase was existed (25.49%) which led to degradation decreases. Furthermore, decreases of TiO_2 surface at 600^{o}C, due to bigger crystalline size, which decreased the active site to degradation of chlorophenol [19]. Calcination at 500^{o}C for 2 hr was found to be optimum temperature and used for study other parameters such as effect of catalyst loading.

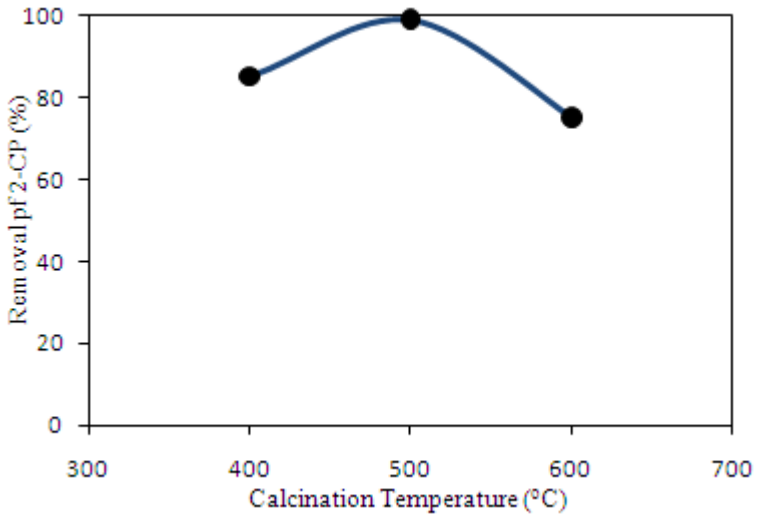

Figure 9. Effect of calcination temperature on photocatalytic removal of 2-CP (50 mg/l, time:90 min).

3.2.3. Effect of loading on TiO_2 nanoparticles activity

The optimum of catalyst loading was studied within the range of 100 to 300mgl^{-1}. Further, the 50 mgl^{-1} a solution of 2-chlorophenol at pH of 6 was used with different loading of TiO_2 catalyst. Fig.10 shows that photocatalytic degradation of 2-chlorophenol increased gradually with loading of TiO_2 nanoparticles up to 200 mgl^{-1} and 99% removal was achieved after 90 min irradiation time. When the loading of TiO_2 catalyst is lower than optimal, the free $^{\bullet}OH$ and $^{\bullet}O_2^-$ superoxide radicals generated is proportionally decreases. At catalyst loading more than optimal, the percentage of degradation was negatively affected due to the scattering of light by excess of catalyst particles was occurred [31, 32]. At the same time, the penetration of light becomes hardly to reaches all the particles due to agglomeration of particles, which reduce the degradation rate [33]. The optimal loading to achieve the best degradation is 200mgl^{-1} and this concentration was tested with different initial concentrations of chlorophenol.

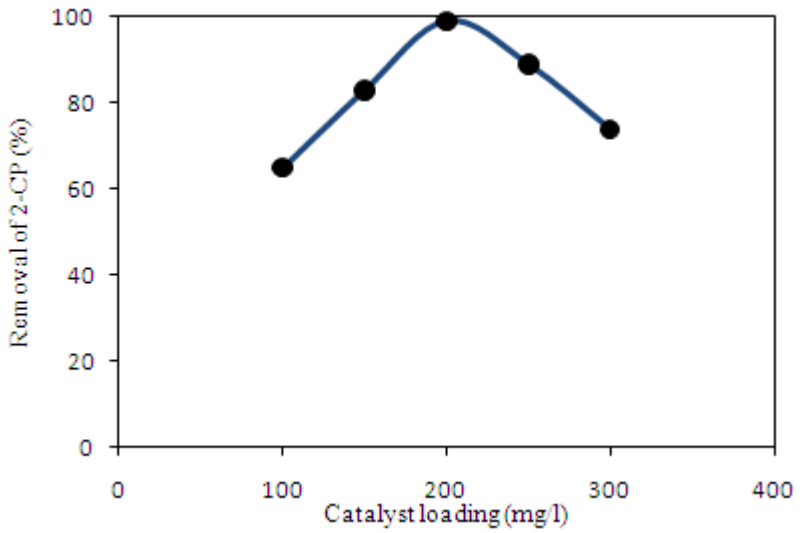

Figure 10. Effect of TiO_2 nanoparticles loading on photocatalytic removal of 2-CP(50 mg/l, time :90 min).

3.3 Solar photocatalytic degradation of cholorophenols by TiO_2 nanoparticles

3.3.1. 2-chlorophenol

In determination of TiO_2 ability as photocatalyst on photodegradation of 2-chlorophenol, several concentrations of 2-chlorophenol were exposed to direct sunlight. The effect of the initial concentration of 2-chlorophenol on photocatalytic degradation process is presented in Fig.11. The degradation efficiency of 2-chlorophenol decreases, when the concentration increased to maximum was observed. At concentration less than 50 mgl^{-1} a complete degradation within 60 min at same conditions of experiment. The removal of 50 mgl^{-1} concentration was achieved at 90 min radiation time. At high concentration such as 100 and 150 mgl^{-1}, the available site on surface of TiO_2 reduces relatively comparing to 2-chlorophenol molecules, in which decreases the degradation rate. However, a

90 and 79 % removal of 2-chlorophenol was achieved when exposure time to direct sunlight about 120 min for 100 and 150 mgl^{-1} initial concentration. At same experimental condition the reduction of initial COD (mgl^{-1}) was evaluated. The removal of COD of 89.6, 75 and 71.6 % were found for 50, 100 and 150 mgl^{-1}, respectively.

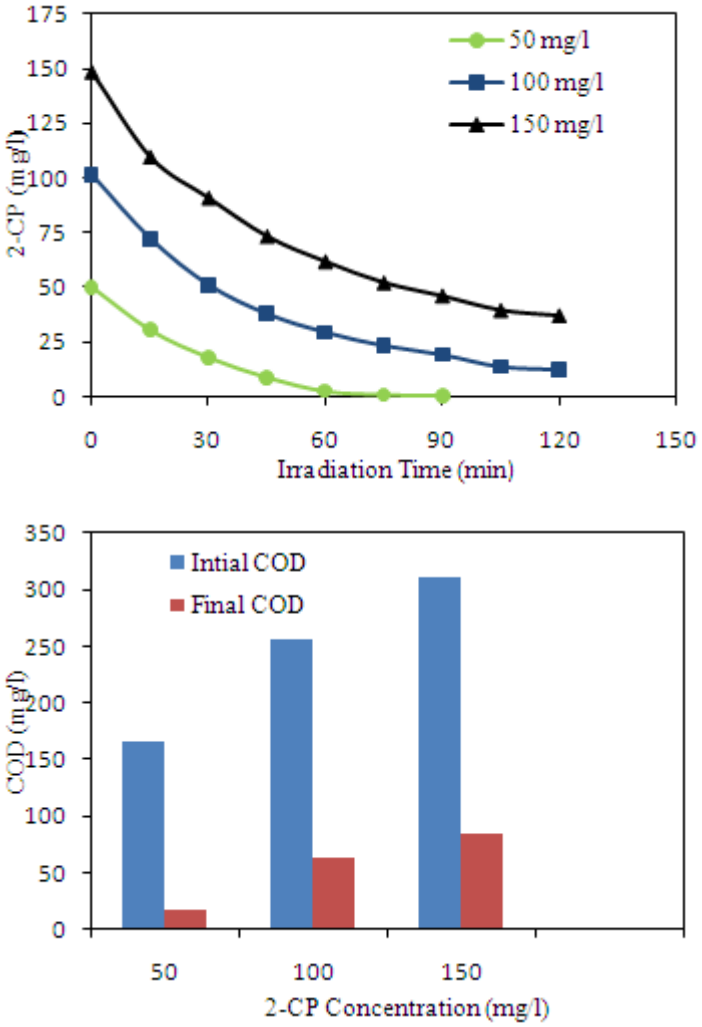

Figure 11. Photocatalytic degradation and COD removal of different initial concentration of 2-CP using the optimum loading of TiO_2 ($2gl^{-1}$), pH at 6, temperature 28-38^oC.

3.3.2 2,4-dichlorophenol

Several initial concentration at varying from 50 to 150 mgl^{-1} were used to investigate the removal of 2,4-dichlorophenol by TiO_2 under same previous conditions. The reduction of 2,4-dichlorophenol removal was observed with increases of initial concentration. A 99 %, 83% and 70 % were found for 50, 100 and 150 mgl^{-1}, respectively within 120 min irradiation time as given in Fig. 12. Lower concentration of 2,4-dichlorophenol indicates easily molecules adsorbed on to surface of TiO_2, which enhanced the removal [16]. At higher concentration of 2,4-dichlorophenol, more molecules covering the surface of TiO_2 which reduces of photon absorption. This result clearly effects on

hydroxyl radicals generation which decreases of removal [34]. At same experimental condition the reduction of initial COD (mgl^{-1}) was evaluated. The removal of COD of 84.5, 68.4 and 60.8 % were found for 50, 100 and 150 mgl^{-1}, respectively.

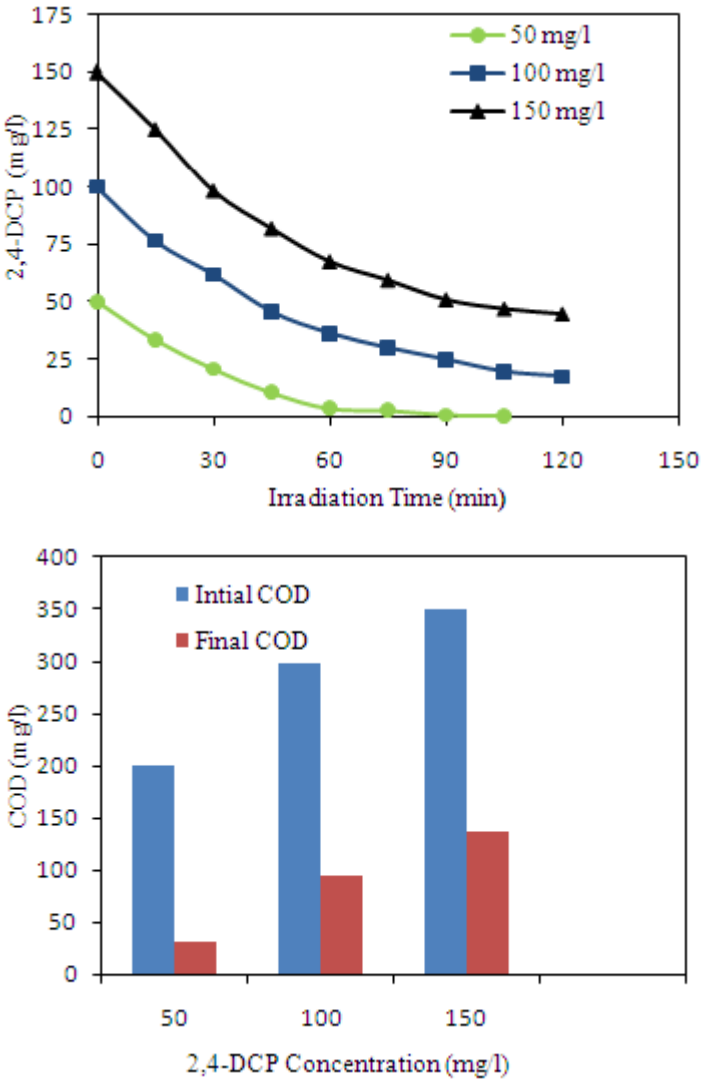

Figure 12. photocatalytic degradation of different initial concentration of 2,4-DCP using the optimum loading of TiO_2, ($2gl^{-1}$), pH at 6 , temperature 28-38^oC.

3.3. 3 2,4,6-trichlorophenol

The photodecomposition rate of 2,4,6-trichlorophenol was influenced by the ability and number of active sites of the TiO_2 catalyst used. The higher removal was observed when the initial concentration of 2,4,6-trichlorophenol is lower as presented in Fig. 13. At $50mgl^{-1}$, can be higher decomposed (96 %) within the 120 min irradiation time. when the concentration increases more than 50 mgl^{-1}, the removal 77 and 65 % were achieved for 100 and 150 mgl^{-1}, respectively within the same time. This observation may be attributed to more and more molecules are adsorbed as multilayer of molecules on the surface of TiO_2 nanoparticle, which was not easily to contact the photogenerated

holes or radicals [35]. On the other hand, the relative number of radicals available for attacking the 2,4,6-trichlorophenol becomes a low in comparison with the number of molecules. At same experimental condition the reduction of initial COD (mgl^{-1}) was measured. The removal of COD of 82.4,64 and 53.6 % were found for 50, 100 and 150 mgl^{-1} initial concentration, respectively.

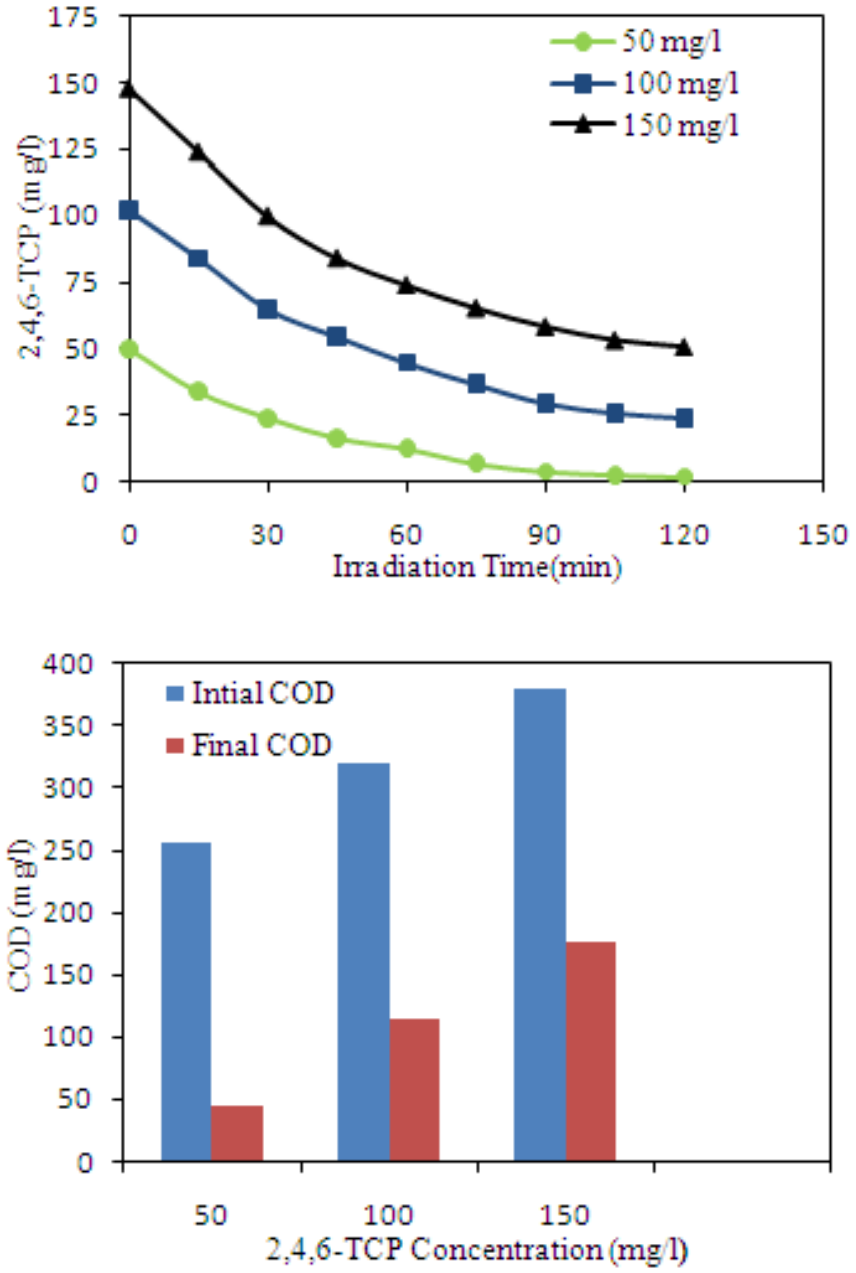

Figure 13. photocatalytic degradation of different initial concentration of 2,4,6-TCP using the optimum loading of TiO_2 ($2gl^{-1}$), pH at 6 , temperature 28-38^oC .

3.4. Kinetic study of chlorophenols degradation by TiO_2 nanoparticle

The kinetics of photocatalytic reactions of chlorophenolic compounds in aqueous solution follows Langmuir-Hinshelwood model:

$$\text{Rate} = -\frac{dC}{dt} = \frac{k_r K_a C}{1+K_a C} = K_{app} C \quad (8)$$

where k_r is the rate constant and K_a is the adsorption equilibrium constant. When the adsorption of chlorophenols on TiO_2 catalyst is relatively weak, the K_a C is insignificant, and the equation can be simplified to the first-order kinetics with an apparent rate constant ($K_{app} = k_r K_a$),

$$\ln \frac{C}{C_0} = -K_{app}\, t \quad (9)$$

The apparent rate constant (k_{app}) evaluated by using Eq.(9), and pseudo-first-order kinetics of chlorophenols degradation was obtained. The apparent rate constants are reported in the Table 2 to show the wide-ranging comparison.

Table 2. Kinetic constants and % removal of chlorophenols degradation by TiO_2 nanoparticle

Compound	2-CP		2,4-DCP		2,4,6-TCP	
Con. mgl^{-1}	Removal % [a]	$K_{app} \times 10^{-2}$ (min^{-1})	Removal % [a]	$K_{app} \times 10^{-2}$ (min^{-1})	Removal % [a]	$K_{app} \times 10^{-2}$ (min^{-1})
50	100	3.69	99	3.28	96	2.41
100	90	2.19	83	1.71	77	1.36
150	79	1.65	70	1.37	65	1.29

[a] removal % after 120 min irradiation time.

The rate constant for lower concentration 50 mgl^{-1} of 2-CP, 2,4-DCP and 2,4,6-TCP are about 3.69×10^{-2} , 3.28×10^{-2} and 2.41×10^{-2} min^{-1} respectively and overall photodegradation rate decreases on order of 2-CP > 2,4-DCP > 2,4,6-TCP . These results indicates that the rate constant reduces in sequence from 2-CP to 2,4,6-TCP, which illustrate difficult attack on the 2,4,6-TCP ring by $HO^{\bullet}$ radical since it an electrophilic reagent. The 2,4,6-TCP has lower solubility property (higher hydrophobicity) than 2-CP and 2,4-DCP. The rate of degradation showed in previous results with observation that faster of rate when chlorophenol hydrophobic property is decreased and increase the solubility [36]. On the other hand, the rate constant decreases of each chlorophenl 2-CP, 2,4-DCP and 2,4,6-TCP when the concentration from 50 to 150 mgl^{-1} was observed. For each chlorophenl such as 2-CP, the rate decreases from 3.69×10^{-2} to 1.65×10^{-2} $min^{-}1$ for concentration from 50 to 150 mgl^{-1}, respectively which attributed to high surface area was available to generate $^{\bullet}OH$ radicals and $^{\bullet}O_2^{-}$ superoxide radicals at lower concentration. At high concentration the TiO_2 photocatalyst surface was covered mainly by chlorophenol molecules and production of $^{\bullet}OH$ and $^{\bullet}O_2^{-}$superoxide radicals were decreased.

4. CONCLUSION

TiO_2 nano-catalyst was prepared by sol-gel method and the structure and morphology were characterized using different techniques. The typical composition of TiO_2 nanoparticles under various calcination temperatures was investigated. The surface area strongly effects by crystal size under various calcinations temperatures. The photocatalytic degradation of 2-CP > 2,4-DCP >2,4,6T-CP was found under pH of 6 , 2 $gl^{-1}$of TiO_2(calcinted at 500^oC) and 2hr direct solar radiation. The photocatalytic degradation process follows the first order reaction of 2 -CP, 2,4-DCP and 2,4,6T-CP with rate constants of 3.69×10^{-2} , 3.28×10^{-2} and 2.41×10^{-2} min^{-1} respectively for 50 mgl^{-1} initial concentration. The rate constant was decreased with concentration more than 50 mgl^{-1} for 2 -CP, 2,4-DCP and 2,4,6T-CP. This study provides a versatile approach for highly efficiency method for the degradation of toxic compounds of poly chlorinated phenol (PCPS) under solar irradiation in the presence of nano-TiO_2 photocatalyst.

ACKNOWLEDGEMENTS
The authors are grateful to the Solar Energy Research Institute (SERI), Universiti Kebangsaan Malaysia and Hadhramout University of Science and Technology, Yemen for their financial support.

References

1. H. Xu, X. Wang and L. Zhang, *Powder Technol*., 185 (2008) 176.
2. O. Harizanov and A. Harizanova, *Sol. Energy Mater. Sol.Cells*,63 (2000) 185.
3. B. Li, X. Wang, M. Yan and L. Li, *Mater. Chem. Phys*., 78 (2002) 184.
4. M. A. Behnajady, N. Modirshahla, M. Shokri, H. Elham and A. Zeininezhad, *J. Environ. Sci. Health. Part A*, 43 (2008) 460.
5. K.-M. Lee, V. Suryanarayanan and K.-C. Ho, *J. Power Sources*, 188(2009) 635.
6. M. Ni, M. K. H. Leung, D. Y. C. Leung and K. Sumathy, *Sol. Energy Mater. Sol.Cells*, 90 (2006) 1331.
7. L. Gu, X.W. Zhang and L.C. Lei, *Ind. Eng. Chem. Res*. 47 (18) (2008) 6809.
8. R.J., Lewis Sr, *Hazardous Chemicals Desk Reference*, 5th ed John Wiley and Sons, New York (2002).
9. K.D. Juan, *Industrial Pollut. Prevention Control*, 3 (1984) 88.
10. Ph. Howard, *Handbook of Environmental Degradation Rates*, Lewis Publishers, MI (1991).
11. R. Schwarzenbach, Ph. Gschwend and D. Imboden, *Environmental Organic Chemistry*, Wiley, New York (1996).
12. D.F. Ollis and H. Al-Ekabi, *Photocatalytic Purification and Treatment of Water and Air*, Elsevier, Amsterdam (1993).
13. M. Pera-Titus, V. Garcia-Molona, M.A. Banos, J.Gimenez and S. Esplu-gas, *Appl. Catal., B.*, 47 (2004) 219.
14. D. Gumy, A. Rincon, R. Hajdu and C. Pulgarin, *Sol. Energy*, 80 (2006) 1376.
15. M. Muruganandham and M. Swaminathan, *J. Hazard. Mater.*, 135 (2006) 78.
16. M. S. Takriff ,M. M. Ba-abbad1, A. A. H. Kadhum1, A. B. Mohamad, K. Sopian, *Adv. Mater. Res.*,233-235 (2011) 3032.
17. APHA, (1989).*Standard method for examination of water and waste water*, 20th ed., American Public Health Association., Washington.

18. J. Wang, W. Suna, Z. Zhang, Z. Jianga, X. Wang, R. Xu, R. Li, X. Zhang , *J. Colloid Interface Sci.*,320 (2008) 202.
19. X. Sun, H. Liu, J. Dong, J. Wei, Y. Zhang, *Catal. Lett*., 135 (2010) 219.
20. H.P. Klug and L.E. Alexander, *X-ray diffraction procedures for polycrystalline and amorphous materials*, Wiley, New York (1997).
21. D. Mardare, M.T asca, M. Delibas and G.I. Rusu, *Appl.Surf.Sci.,* 156 (2000) 200.
22. L.Q. Jing, Z. L. Xu, X. J. Sun, J. Shang and W.M. Cai, *Appl Surf Sc.i,* 180(2001)308.
23. Z.L. Xu, J. Shang and C.M. Liu, *Mater. Sci Eng. B,* 63(1999) 211.
24. L. wan, Y. Gao. X. Xia, Q. Deng and G.Shao, *Mater. Res. Bull.*,46 (2011) 442.
25. J. Garca-Serrano, E. Gómez-Hernandez, M. Ocampo-Fernandez and U. Pal, *Curr. Appl Phys.*, 9 (2009) 1097.
26. E. Ziegler, A. Heinrich, H. Oppermann and G. Stover, *Phys. Status Solidi A*, 66 (1981) 635.
27. Z. Ambrus, N. Bala´zs, T. Alapi and G. Wittmann, P. Sipos, A. Dombi and K. Mogyorosi, *Appl. Catal., B.*, 81 (2008) 27.
28. B. Neppolian, H. Jung and H. Choi, *J. Adv. Oxid. Technol*.,10 (2007) 369.
29. M.A. Barakat, H. Schaeffer, G. Hayes and S. Ismat-Shah, *Appl. Catal., B.*,57 (2005) 23.
30. S. Sakthivel, M. C. Hidalgo, D. W. Bahnemann, S. U. Geissen, V.Murugesan and A. Vogelpohl, *Appl. Catal., B.*, 63(2006)31.
31. L. Rideh, A. Wehrer, D. Ronze and A. Zoulallian, *Ind. Eng. Chem. Res*., 36, (1997) 4712.
32. S. Lathasree, R.A. Nageswara, B. Sivasnkar, V. Sadasivam and K. Rengaraj, *J. Mol. Catal. A: Chem.,* 223 (2004) 101.
33. R.A. Doong and W.H. Chang, *J. Photochem. Photobiol. A: Chem*., 116 (1998) 221.
34. T. Velegraki and D. Mantzavinos, *Chem. Eng. J.,* 140 (1–3) (2008) 15.
35. S.K. Pardeshi and A.B. Patil, *J. Hazard. Mater.*,163 (2009) 403.
36. J. Bandara, J.A. Mielczarski, A. Lopez and J. Kiwi, *Appl. Catal., B.*, 34(2001) 321–333.